International Journal of Physics
and Research (IJPR)
ISSN (P): 2250–0030; ISSN (E): 2319–4499
Vol. 13, Issue 1, Jun 2023, 1-10

TRANS STELLAR
•Journal Publications •Research Consultancy

STRUCTURAL, OPTICAL, ELECTROCHEMICAL PROPERTIES OF NANO GRAPHENE OXIDE/NIO NANO COMPOSITE SUITABLE FOR SUPER CAPACITOR APPLICATIONS.

D.PREMANAND[1], M. SAPPANI MUTHU[2], J. AGNES[3], P.AJITH[4], M.S. SELVAKUMAR[5] & M. PRESHETH[6]

[1,2,3,4]*Materials Research Centre, Dept. of Physics, St. Xavier's College (Autonomous), Palayamkottai- 627002, Tamilnadu, India*

[5,6]*Dept. of. Chemistry, St. Xavier's College (Autonomous), Palayamkottai- 627002, Tamilnadu, India*

Affiliated to Manonmaniam Sundaranar University, Abishekapatti 627012, Tirunelveli, Tamilnadu, India

ABSTRACT

In this paper, NiO nanoparticles Graphene sheet was prepared by hydrothermal synthesis method, which is one of the simplest techniques. The prepared NiO nanoparticles graphene sheets were characterized, and XRD analysis confirms the crystallinity and phase purity of the sample. There is a band gap between the UV and visible spectra of the sample at 3.25 ev. Mesoporous morphology of the material was discovered through SEM micrographs. This mesoporous morphology may be due to an increase in the material's surface-to-mass ratio, which may increase the material's specific capacitance. The electrochemical performance of the as-prepared nanocomposite materials was measured. The CV-Cyclic voltammetry GO/NiO nanocomposite. Its shows that at a current density of 0.5 Ag^{-1}, the capacitor exhibits a higher specific capacitance of 707.56 Fg^{-1} and is a suitable material for electrode application in a super capacitoras described.

KEYWORDS: Nano Composite, Nickel Oxide, Graphene Oxide, Super Capacitor Application.

Received: Jun 03, 2022; **Accepted:** Jun 23, 2022**; Published:** Jul 25, 2023; **Paper Id:** IJPRJUN20231

Original Article

INTRODUCTION

There is an increase in the demand for conventional energy sources due to the rising demand for energy consumption on the planet today. As a result, the entire world has focused on energy-related research. A renewable energy source is the best option for energy. This type of energy's main drawback is that it is not always accessible. As a result, when this type of energy is available, it must be stored so that it can be used when needed [1]. Li-ion batteries and super capacitors are common forms of energy storage [2-4]. Metal oxides such as a SnO_2, Fe_3O_4, Fe_2O_3, CO_3O_4, RuO_2, MoO_3, ZnO, CuO, and WO_3have been developed as a promising super capacitor electrode material [7-27]. NiO-based nanostructures have been widely used as electrode components for electrochemical super capacitors, fuel cells, electronic films, gas sensors, and lithium-ion batteries [30]. For high-performance electrochemical super capacitor applications, NiO has merited and continues to merit significant research efforts. Because it is less expensive and easier to process using a variety of methods. The Nickel Oxide (NiO) semiconductor has a P-type band gap (3.6 to 4.9 eV) and is highly chemically stable and electron transferable. [1] Graphene can be used to improve the electrical conductivity of materials. This is very useful for improving the electrochemical properties of nickel oxide electrodes. The material used in this investigation is a nickel

oxide/graphene oxide nanocomposites prepared by hydrothermal processes as a pseudo-capacitive electrode. [6, 7] In devices, nickel oxide/graphene oxide nanocomposite has been investigated for its optical, thermal, and electrochemical properties. Using cyclic voltammetry and EIS techniques, the electrochemical properties of nickel oxide and graphene oxide nanocomposites were investigated.[8] The nanocomposite is constructed to enhance suitable for super capacitor applications.[9]

EXPERIMENTAL

Materials and Method

Graphite Flake powder (FG), sulfuric acid (H_2So_4), potassium permanganate ($KMnO_4$), sodium nitrate ($NaNo_3$), hydrogen peroxide (H_2O_2), Hydrochloric acid (HCL), Ethanol, and Nickel Acetate $C_2H_6NiO_4$. $4H_2O$

Synthesis of Graphene Oxide (GO)

The process of producing graphite oxide (GO) was described in detail using a modified Hummers method. Graphite (FG) powder (1.5g), sodium nitrate (3.0g), and $NaNO_3$ were combined in the flask before cooling on an ice bath and stirring for 45 minutes. Concentrated H_2So_4 (70ml) was then added.The potassium permanganate $KMnO_4$ (9.0g) was slowly added while the temperature remained below 293 k. After stirring in an ice bath for two hours, the mixture was transferred to a water bath and kept at 308 degrees Celsius for one hour. The mixture was then given 140 ml of water, which caused it to slowly rise to 371 k and stay there for 1 hour. The reaction's temperature was discovered to rapidly rise. With effervescence, the colour of the reaction changed to brown, and the reaction temperature increased quickly to 373 k. The colour of the aforementioned solution changed to yellow after 30 ml of H_2O_2 was added. A solution of water and HCL was used to wash the solid mixture and dried at 323k for 96 hours after filtration and centrifugation at 6000 rpms. After sonicating GO (50mg) in ethanol (65ml) for 3 hours, the Nickel Acetate $C_2H_6NiO_4$. $4H_2O$ powder was added to the solution in a 50:50 mass percent ratio and ultrasonically dispersed for 1 hour. The suspension was sealed in a Teflon-lined autoclave (100ml) and heated at 473 k for 12 hours. The finished products underwent filtering, an ethanol wash, and 24-hour vacuum drying at 323 k. For comparison, the above method yielded pure NiO and graphene sheets (GS).

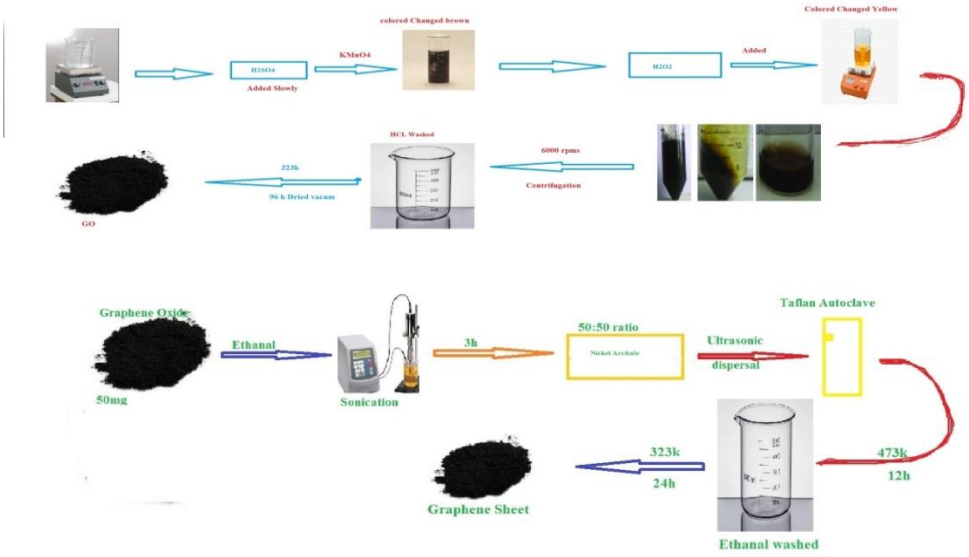

Figure 2.1: Synthesis of Graphene Oxide/NIO

CHARACTERIZATION

The crystallographic structure of Graphene/ NiO Nanocomposites was determined by an X-ray diffraction system PAN analytical Expertinstrument equipped with CuKa (λ=1.5406A) radiation. UV- Ultraviolet –visible spectroscopy, CV-electrochemical work station of cyclic voltammetry.

RESULT AND DISCUSSION

XRD Analysis

The most common X-ray powder diffraction analysis is used to characterize the structure of crystalline and nanomaterials, allowing for atom-by-atom comparisons and also verifying the oxidation status of crystals and nano-crystals. As shown in Figure 4.1a, an X-ray diffraction analysis of nanographene oxide was performed. This analysis is based on the Debye-Scherer equation which determines the size of graphene oxide nanoparticles' typical crystals D.

$$D=0.89\ \lambda/\beta \cos\theta$$

The Braggs angle diffraction of full width at half maximum of incident beam's wavelength (λ =1.5406), the average particle size of 21nm found in the study. One can verify peak structure by comparing them to standard available data, 15.15º,19.59º,21.83º, 24.83º,27.06º,32.92º,43.75º,45.55º,55.89º,XRD patterns. As we can see, there is a prominent peak at 27.06º that corresponds to a prominent plane. The full width maxima prominent planes of the 2 θ value. From peak 21.51º, we can observe a sharp peak, and at peak 27.06°, an intense peak. There are all peaks in these graphite oxide nanoparticles that fit well with their good interlayer structure. This interlayer facing greater than value is graphite powder, according to the peak at2 θ =70º. As a result of oxygenated functional groups and the interrelationship between water molecules, the spectrum contains oxygenated functional groups. There is diffraction due to oxinated graphite at 2 θ = 27.06ºan interlayer structure and highly organized structure are evidenced by nanographene oxide diffraction peak around 27.06°.It is estimated that the 55.89° peak disappeared and was replaced by 45.56°, indicating that the crystalline lattice of nanographene oxide was de-spaced after chemical oxidation and exfoliation. It has been found that the XRD patterns of nanographene oxide the crystalline structure of nanographene oxide conform to tetragonal hausmannite nanoparticles. [1,2]The second layer of Figure 4.1 b. shows the XRD spectrum of Nickel oxide/graphene sheets. The diffraction peaks at 37.6°, 43.7°, and 63.9°, are NiO which are in accordance with the **JCPDS data for NiO (card no; 47-1049)** and the peaks around at 2 θ=37.7°, 43.7°, and 63.7° were identified as [111],[200]and [220] respectively. From the XRD spectrum, there is no distinctive peak of graphene oxide (2 θ =10.9°) or graphite flakes (2 θ =21.6°) confirming that graphene oxide was well condensed [37]. There was no difference between graphene and the composite at about 26°, which corresponds to the d-spacing of 0.36nm. NiO nanocrystalline is not greatly affecting the origin of graphene as the d-spacing is higher than that of graphite (0.33nm), suggesting that the NiO nanocrystalline has little effect on natural graphite. [38].

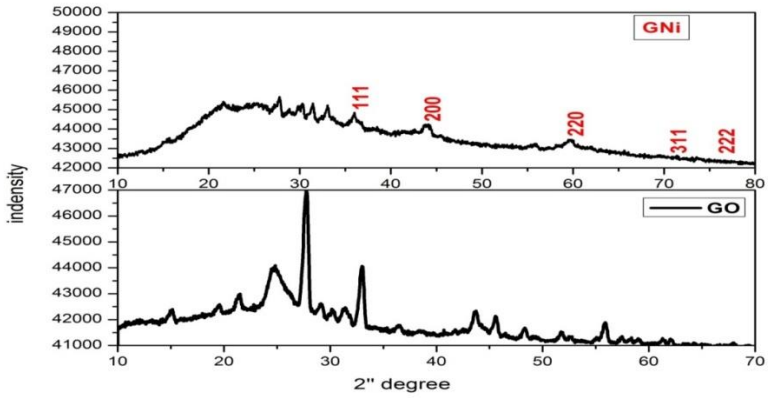

Figure 4.1: XRD Pattern of Nano Graphene Oxide and NiO Nanocomposite

UV-Vis NIR Analysis

UV- Visible spectra of Nickel oxide/graphene sheet is shown in Figure 4.2.b. In the UV-visible spectrum, there are two characterization absorption bands. The centered band absorption at 271 nm is attributed to $\pi \rightarrow \pi *$ C-C aromatic transitionbands. The shoulder centered at 298 nm corresponds to $n \rightarrow \pi *$ transitions of C=O bonds. The spectra show that the absorption increases steadily and eventually reaches a constant value. The absorption peak at 323 nm is also red shifted to 271 nm, and the other absorption band at 296 nm is completely removed. According to UV-visible spectra, most of the oxygen-containing functional groups have been removed from the graphene's surface, and electronic conjugation has been reduced a lot. Nano sheets can now be synthesized solvothermally. Also, we got similar results by Yu et al[41] andXu et al[42].The NiO band gap of graphene sheets nanocomposite was then calculated using the Tauc relation. [43],

α(αhν) n = A (hν - Eg)Where α,A,h,ν, n(=1/2)

An optical absorption coefficient and a direct band gap and the planks constant are all values for the optical absorption coefficient and the planks constant. Graph's straight region between and was used to calculate the band gap energy hv and $(\alpha hv)^2$ the results show that the band gap energy was found to be 3.25ev as shown in Fig. 4.2 a.

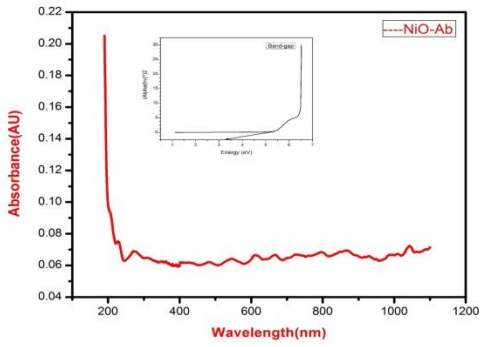

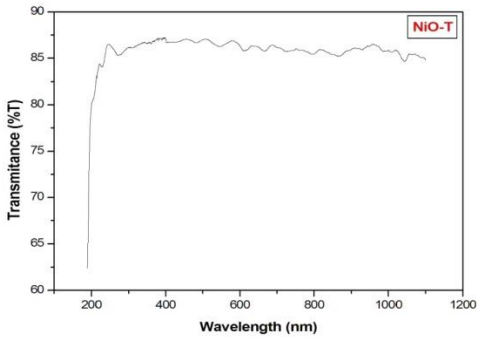

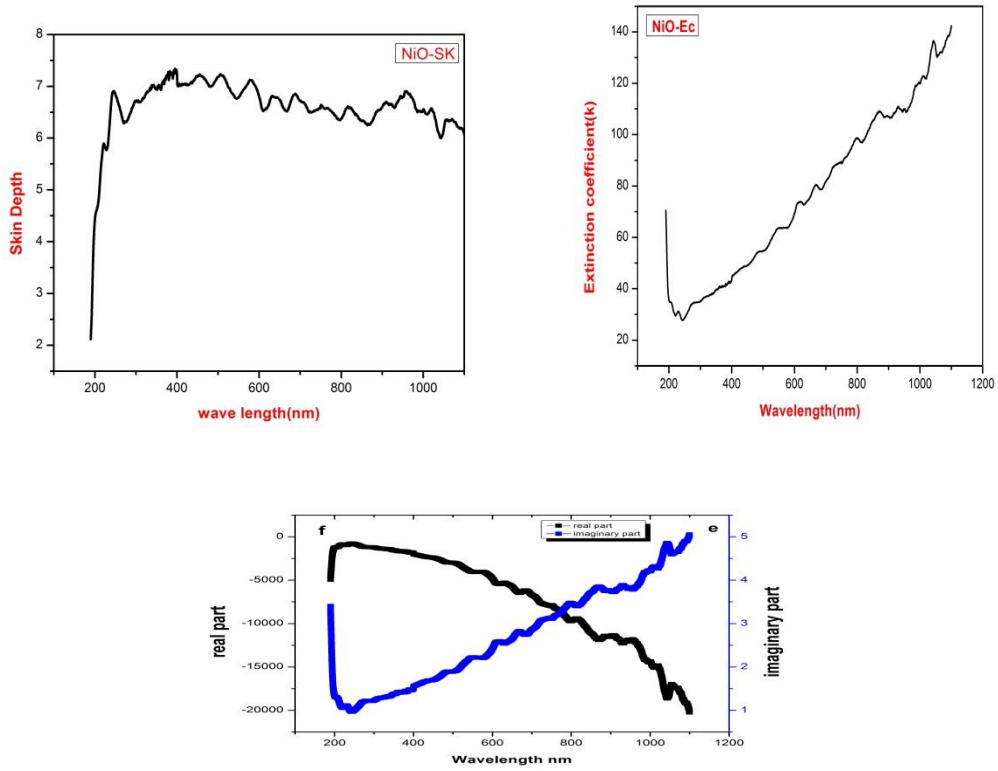

Figure 4.2 a) Absorption and Tauc's Plot, b) Transmittance, c) Skin Depth, d) Extinction Coefficient.e) Dielectric Constant

Skin Depth

The optical penetration depth of a substance can pass through it. Skindepth$\delta=^{1}/\alpha$, as shown in Figure 3.2(c) the skin depth increases up to 246 nm and then decreases. Approximatelyvalue 6 mm was found to be the minimum value of skin depth308 nm and then began to climb until it reached its maximum at 387 nm. As a result, electromagnetic radiation with a wavelength of around 398 nm penetrates deeper into the substance.

Extinction Coefficient

The degree to which a chemical species or material absorbs light at a specific wavelength. The chemical structure of the material produced the electromagnetic radiation absorption scattering loss of materials. $K=^{a\lambda}/4M$, fromFigure 4.3(d) With wavelength increasing after 244nm, the extinction coefficient decreases, then increases after 890nm, where it goes linear or becomes constant. Optical properties of UV-Visible Spectrum.

Dielectric Constant

An investigation of the relationship between permittivity, polarizability, and density is conducted using the Dielectric Constant calculation. The Real part of the dielectric constant gives information about the speed of light so that the material can be slowed down. The fictitious portion represents energy absorption by a dipole in an electric field.

Dielectric Constant Real Part$A=\pi r^2=n^2-k^2$

Imaginary part $\varepsilon_i=2nk$

Refractive Index K–Extinction coefficient

Figure 4.2.(e). The fluctuation of imaginary real components of the constant dielectric has an opposing tendency, as shown by the Dielectric Constant of the produced sample. The greatest value of the real part is at 242 nm, indicating the most absorption, while the minimum value is at 1098 nm. Similarly, the imaginary part has a maximum value of 1100 nm, indicating the highest absorption, and a minimum value of 243 nm.

Electrochemical Analysis

The electrochemical test was performed in a three electrode system using a potentio start at room temperature. We used a glassy carbon disc of diameter 5mm as the electrode. The prepared ink was dropped onto the working electrode. To achieve a smooth texture, the glassy carbon electrode was polished with 0.3 micrometer thick powdered alumina. If was raised ultrasonically in a mixture of ethanol and water, followed by the addition of 5mg of the catalyst. Notion was used as the binding agent Graphite rod and mercury oxide are the counter and reference electrodes used for the experiments. The electrochemical activity of the as-prepared sample was studied using CV and LSV. The LSV was recorded to evaluate ORR offset potentials and kinetics. In addition to that, K-L plot was drawn with different rotation speeds at a scanning speed of $5ms^{-1}$. CV was determined for a potential of 10000 cycles in an alkaline medium. The OH tolerance of the catalyst was determined with LSV at a scan speed of 5mV/sec. Rotating disc electrode experiments were performed to measure the percentage peroxide. To set the RRDE as a working electrode, a total of 20ml of the catalyst clash was coated on a GC disc and then was dried at room temperature.*(Sivalingam Ramesh et al. 2018; SrinuAkula et al. 2020)*

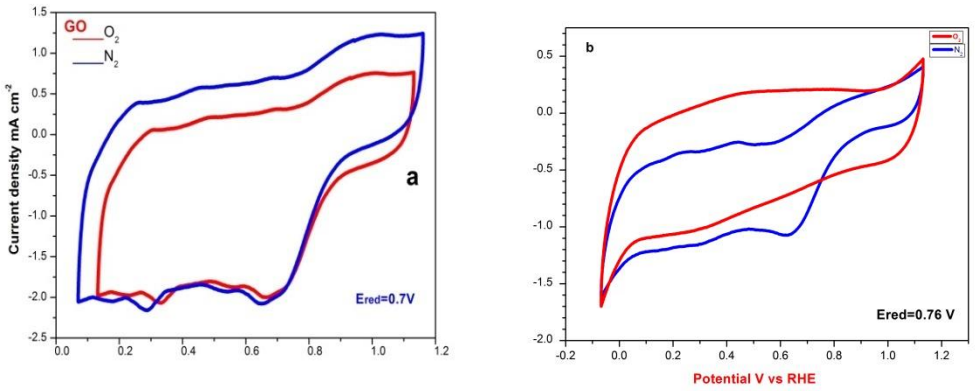

Figure 3.1 a) Nano Graphene Oxide

b) Nano Graphene Oxide /Nickel Oxide nanocomposite for electrochemical analysis.

A three-electrode system was used to compare the electrochemical properties of GO/NiO nanocomposite. The electrochemical reaction between GO and NiO was also examined. An analysis of the CV curves of the bare GO/NiO nanocomposite. A CV curve was measured for an electrode within the potential range of -0.2V to 1.2V. The CV curve of the bare GO electrode is shaped like a rectangle and does not have any redox peaks. There is pseudo capacitance in the capacitance of GO nanosphereelectrodes. As shown in figure 3.1(b), pristine NiO active electrodes have CV diagrams. Over the voltage range of -0.2-1.2 v, all CV curves showed redox peaks at a scan rate of 5 mV, indicating pseudo capacitive response and significant rate capability. As the scan sweep is increased, the areas of redox peak current intensity become larger. A drop in resistance and an increase in electron and ion transfer rates contributed to the cathodic peaks shifting towards a negative potential (-Ve). NiO electrode material morphology and chemical composition Reversible

faradaic redox reactions and redox reactions that produce potassium hydroxide (KOH) could be closely correlated to the strong peaks. Figure 3.1 b) at a scan rate of 5 mV/s, the plots appear to be CV plots of GO/NiO nanocomposite. A composite electrode's CV curve exhibits relatively obvious redox peaks, which are explained by the typical pseudocapacitive behaviour of a GO electrode.

Using the formula provided, the specific capacitance of the sample can be calculated. Cp = A/2mk (V_2-V_1), where A is the area with units within the curve. The active material's mass is m, the CV (50) scan rate in volts per second is k, and the CV potential window is (V_2-V_1) (0.99). In table 3.2, the specific capacitance was calculated.

Sample	Saturated Solution	Area	Specific Capacitance F/G
Nano Graphene Oxide (GO)	O_2	0.0615978	615.978
Nano Graphene Oxide (GO)	N_2	0.0423410	423.410
Nano Graphene Oxide (GO) / Nickel oxide (NiO) Nanocomposite	O_2	0.0243054	243.054
Nano Graphene Oxide (GO) / Nickel oxide (NiO) Nanocomposite	N_2	0.7078653	707.865

A relation is used to measure the specific capacitance values of GO/NiO nanocomposite. In comparison to their individual compounds of bare GO and NiO electrode material, the measured specific capacitance values of the GO/NiO electrodes are significantly higher. Composites with a larger surface area are created by wrapping GO spherical nanoparticles on NiO nanoparticles, which improves the specific capacitance of the GO/NiO electrode.

Comparative study of Nano Graphene Oxide (GO) or Nickel Oxide (NiO) Based Super Capacitor Composites using Various Methods and Nanostructures.

Compounds	Method	Nanostructures	Electrolyte	Specific Capacitance	Reference
CuO/MnO_2	Hydrothermal	Diatom	1 M $Na_2 SO_4$	240 F/g at 0.5 Ag^{-1}	15
MnO_2/NiO	Hydrothermal	Spherical	1 M KOH	247 F/g at 0.5 A/g	16
CuO/ Co_3O_4	Hydrothermal	Nano sheet	5 M KOH	246 F/g at (A/g)	17
MnO_2/CuO	Hydrothermal	Spherical	1M KOH	279.12 F/g at 0.5 A/g	14
NiO-Rgonanosheets	Electrostatic self-assembly annealing	Nano sheets	1 M NaOH	686 F/g at 1 Ag^{-1}	09
NiO-MnO2 & reduced graphene oxide	Microwave assisted method	Spherical	0.1 M KOH	596 F/g at 1Ag^{-1}	10
GO/NiO Nanocomposite	Hydrothermal	Nano sheet	1 M KOH	707.86 F/g at 0.5A/g	**Present work**

The specific capacitance performance of nanographene oxide (GO) and nickel oxide (NiO) nanocomposite (GO/NiO) was compared in the current study, which showed that the latter had better cycling performance than some previously published papers.

CONCLUSIONS

A Nano Graphene oxide/Nickel oxide nanocomposite was successfully synthesized by a hydrothermal process. The results are obtained from the optical properties of absorption coefficient, dielectric constant; the GO/NiO nanocomposite has an electrochemical properties specific capacitance value calculated at 707.86 F/g at 0.5 A/g.

ACKNOWLEDGEMENTS

The authors would like to express their heartfelt gratitude to Rev. Dr. S. Mariadoss S.J., principal of St. Xavier's College, Palayamkottai, and Rev. Dr. G. Pushparaj S.J., secretary of St. Xavier's College, Palayamkottai.

REFERENCES

1. *Varshney, B., Siddiqui, M. J., Anwer, A. H., Khan, M. Z., Ahmed, F., Aljaafari, A., &Azam, A. (2020). Synthesis of mesoporous SnO 2/NiO nano composite using modified sol–gel method and its electrochemical performance as electrode material for supercapacitors. Scientific reports, 10(1), 1-13.*
2. *Singh, A., & Chandra, A. (2013). Graphene and graphite oxide based composites for application in energy systems. physica status solidi (b), 250(8), 1483-1487.*
3. *Luo, X., Wang, J., Dooner, M., & Clarke, J. (2015). Overview of current development in electrical energy storage technologies and the application potential in power system operation. Applied Energy, 137, 511-536.*
4. *Arico, A. S., Bruce, P., Scrosati, B., Tarascon, J. M., & Van Schalkwijk, W. (2011). Nanostructured materials for advanced energy conversion and storage devices. Materials for sustainable energy: a collection of peer-reviewed research and review articles from Nature Publishing Group, 148-159.*
5. *Chandra, A., Roberts, A. J., Yee, E. L. H., & Slade, R. C. (2009). Nanostructured oxides for energy storage applications in batteries and supercapacitors. Pure and Applied Chemistry, 81(8), 1489-1498.*
6. *Yu, Z., Tetard, L., Zhai, L., & Thomas, J. (2015). Supercapacitor electrode materials: nanostructures from 0 to 3 dimensions. Energy & Environmental Science, 8(3), 702-730.*
7. *Manikandan K, DhanusKodi S, Maheswari N, Muralidharao G. AIP. Confe. Proc.1731,50048 (2016)*
8. *Xu, S., You, L., Zhang, P., Zhang, Y., Guo, J., & Wang, C. (2013). Fe 3 O 4@ coordination polymer microspheres with self-supported polyoxometalates in shells exhibiting high-performance supercapacitive energy storage. Chemical Communications, 49(24), 2427-2429.*
9. *Liu, M., Zhou, L., Luo, X., Wan, C., &Xu, L. (2020). Recent advances in noble metal catalysts for hydrogen production from ammonia borane. Catalysts, 10(7), 788.*
10. *Sun, H., Chen, B., Jiao, X., Jiang, Z., Qin, Z., & Chen, D. (2012). Solvothermal synthesis of tunable electroactive magnetite nanorods by controlling the side reaction. The Journal of Physical Chemistry C, 116(9), 5476-5481.*
11. *Xia, H., Hong, C., Li, B., Zhao, B., Lin, Z., Zheng, M., &Aldoshin, S. M. (2015). Facile synthesis of hematite quantum-dot/functionalized graphene-sheet composites as advanced anode materials for asymmetric supercapacitors. Advanced Functional Materials, 25(4), 627-635.*
12. *Lee, K. K., Chin, W. S., & Sow, C. H. (2014). Cobalt-based compounds and composites as electrode materials for high-performance electrochemical capacitors. Journal of Materials Chemistry A, 2(41), 17212-17248.*
13. *Varshney, B., Siddiqui, M. J., Anwer, A. H., Khan, M. Z., Ahmed, F., Aljaafari, A., &Azam, A. (2020). Synthesis of mesoporous SnO_2/NiO nano composite using modified sol–gel method and its electrochemical performance as electrode material for supercapacitors. Scientific reports, 10(1), 1-13.*
14. *Park, J. H., Ko, J. M., & Park, O. O. (2003). Carbon nanotube/RuO2 nanocomposite electrodes for supercapacitors. Journal of the Electrochemical Society, 150(7), A864.*
15. *Gujar, T. P., Shinde, V. R., Lokhande, C. D., Kim, W. Y., Jung, K. D., &Joo, O. S. (2007). Spray deposited amorphous RuO2*

for an effective use in electrochemical supercapacitor. Electrochemistry communications, 9(3), 504-510.

16. *Chang, K. H., & Hu, C. C. (2004). Hydrothermal synthesis of hydrous crystalline RuO2 nanoparticles for supercapacitors. Electrochemical and Solid State Letters, 7(12), A466.*
17. *Xue, J., Wu, T., Dai, Y., & Xia, Y. (2019). Electrospinning and electrospunnanofibers: Methods, materials, and applications. Chemical reviews, 119(8), 5298-5415.*
18. *Lu, T., Pan, L., Li, H., Zhu, G., Lv, T., Liu, X.,...& Chua, D. H. (2011). Microwave-assisted synthesis of graphene–ZnOnanocomposite for electrochemical supercapacitors. Journal of Alloys and Compounds, 509(18), 5488-5492.*
19. *Zhao, B., Xu, J., Liu, Y., Fan, J., & Yu, H. (2021). Amino group-rich porous g-C3N4 nanosheetphotocatalyst: Facile oxalic acid-induced synthesis and improved H2-evolution activity. Ceramics International, 47(13), 18295-18303.*
20. *Xue, C., Lv, Y., Zhang, F., Wu, L., & Zhao, D. (2012). Copper oxide activation of soft-templated mesoporous carbons and their electrochemical properties for capacitors. Journal of Materials Chemistry, 22(4), 1547-1555.*
21. *Varshney, B., Siddiqui, M. J., Anwer, A. H., Khan, M. Z., Ahmed, F., Aljaafari, A.,...&Azam, A. (2020). Synthesis of mesoporous SnO_2/NiO nano composite using modified sol–gel method and its electrochemical performance as electrode material for supercapacitors. Scientific reports, 10(1), 1-13.*
22. *Miskei, M., Gregus, A., Sharma, R., Duro, N., Zsolyomi, F., &Fuxreiter, M. (2017). Fuzziness enables context dependence of protein interactions. FEBS letters, 591(17), 2682-2695.*
23. *Lang, J. W., Kong, L. B., Wu, W. J., Luo, Y. C., & Kang, L. (2008). Facile approach to prepare loose-packed NiO nano-flakes materials for supercapacitors. Chemical Communications, (35), 4213-4215.*
24. *Liang, K., Tang, X., & Hu, W. (2012). High-performance three-dimensional nanoporous NiO film as a supercapacitor electrode. Journal of Materials Chemistry, 22(22), 11062-11067.*
25. *Poizot, P. L. S. G., Laruelle, S., Grugeon, S., Dupont, L., &Tarascon, J. M. (2000). Nano-sized transition-metal oxides as negative-electrode materials for lithium-ion batteries. Nature, 407(6803), 496-499.*
26. *MacLachlan, M. J., Coombs, N., Bedard, R. L., White, S., Thompson, L. K., &Ozin, G. A. (1999). Mesostructured metal germanium sulfides. Journal of the American Chemical Society, 121(51), 12005-12017.*
27. *Wang, X., Song, J., Gao, L., Jin, J., Zheng, H., & Zhang, Z. (2004). Optical and electrochemical properties of nanosized NiO via thermal decomposition of nickel oxalate nanofibres. Nanotechnology, 16(1), 37.*
28. *Vehmeijer, F. O., Küpers, L. K., Sharp, G. C., Salas, L. A., Lent, S., Jima, D. D.,...& Felix, J. F. (2020). DNA methylation and body mass index from birth to adolescence: meta-analyses of epigenome-wide association studies. Genome medicine, 12(1), 1-15.*
29. *Fantini, M. C. A., Ferreira, F. F., &Gorenstein, A. (2002). Theoretical and experimental results on Au–NiO and Au–CoOelectrochromic composite films. Solid State Ionics, 152, 867-872.*
30. *Mozetič, M., Vesel, A., Primc, G., Eisenmenger-Sittner, C., Bauer, J., Eder, A.,...&Montelius, L. (2018). Recent developments in surface science and engineering, thin films, nanoscience, biomaterials, plasma science, and vacuum technology. Thin Solid Films, 660, 120-160.*
31. *Sivaraj, M., et al. "Effect Of Particle Size Distribution And Mixing Homogeneity On Microstructure And Hardness Of Sintered Al-Tic Nano Composites." International Journal of Mechanical and Production Engineering Research and Development 10.3 (2020): 10873-10882.*

32. *Jindal, H. I. M. A. N. S. H. U., I. S. Sandhu, and M. Chitkara. "A reduced graphene oxide electrode for solid-state hydrogen storage within a proton battery." International Journal of Mechanical and Production 9.4 (2019): 659-670.*

33. *Bhattacharya, S. S., and S. B. Chaudhari. "Study on structural and thermal properties of polypropylene silica nanocomposite filaments." International Journal of Textile and Fashion Technology 5.1 (2015): 15-22.*

34. *Satyanarayana, K. R., B. SURENDRA BABU, and B. RAMESH CHANDRA. "Microstructurural characterization of 6063 aluminium alloy nano-composites." International Journal of Mechanical and Production Engineering Research and Development 8.2 (2018): 851-856.*